Short repulsive binary-alloy chains as a model for disordered quantum wells

R. Rey-Gonzalez* and P. A. Schulz
Instituto de Física Gleb Wataghin, Universidade Estadual de Campinas, 13083-970 Caixa Postal 6165 Campinas, São Paulo, Brazil
(Received 24 September 1997)

Quantum confinement in one-dimensional disordered quantum wells is verified by means of resonant tunneling signatures in the transmission probability of an electron through barrier-well-barrier structures. The wells are simulated by short repulsive binary-alloy chains. These chains are interesting disordered systems, showing both localized and delocalized states. Bona fide confined states in the energy range where the bulk chain presents states with a localization length that exceeds at least three times the quantum-well width are found. These bona fide quantum-well states show clear symmetry properties for the envelope probability density in spite of disorder. In addition, the inadequacy of mean-field approximations to understand the quantization rules of disordered heterostructures is discussed. [S0163-1829(98)01123-0]

I. INTRODUCTION

Quantum confinement effects in quantum wells of crystalline semiconductors are well documented in the literature and are a direct consequence of the interference of spatially extended wave functions in these systems.[1] However, the situation is rather different for heterostructures based on disordered materials, where the electronic and optical properties remain unclear. Indeed, these properties give no direct answer to the question of whether quantum confinement effects exist or not in these systems. A paradigmatic example of this situation is given by the properties of amorphous semiconductor-based heterostructures. Miyazaki, Ihara, and Hirose[2] analyzed tunneling properties of an ultrathin amorphous silicon layer sandwiched by silicon nitride barriers: currents bumps in the I-V characteristic curve are associated to resonant tunneling effects through the double barriers. Alvarez and collaborators had measured negative conductance in a-SiC:H/a-Si/a-SiC:H structures that they related to quantum size effects.[3] However, these results are not conclusive. Also, optical and photothermal measurements in a-Si superlattices have shown results that can be attributed to the spatial confinement.[4,5] These works have in common the use of the effective-mass approximation as an interpretation framework,[2–5] while from a theoretical point of view this problem has been addressed both by using microscopic models for disorder[6–9] or some mean-field averaging procedure[10] or an effective-mass approximation.[11]

In this work we show the necessity to go beyond a mean-field approximation, such as effective-mass or virtual-crystal (VCA) approximations when correlations are imposed on disorder. Correlations lead to a description of these systems including inherently a key feature of many disordered bulk materials: the presence of well defined energy ranges showing either localized or delocalized states. A useful framework for a model quantum well with these characteristics is given by a number of disordered one-dimensional (1D) systems exhibiting nontrivial extended states, according to recent theoretical investigations.[12–24] Having this scenario in mind, one could build a quantum well with a finite segment of a linear disordered chain of this class: a repulsive binary alloy.[14] Since there are energy ranges showing either localized or delocalized states, one can directly monitor the spatial quantization as a function of the localization of the bulk states of the quantum-well material.

On the other hand, the use of the mean-field approximation for describing quantum confinement effects in disordered materials is questionable when correlations are present, as in our model, since a correlated disordered material presents resonances that cannot be handled within mean-field or effective-mass approximation frameworks.

Here, we report on the electron resonant tunneling through a double-barrier disordered quantum well (DB-DQW), the existence of quantized levels in the disordered well layer as a function of delocalization of states in the corresponding bulk chain, and the importance of microscopic models in opposition to effective potentials for disordered quantum wells. As a consequence, the present quantized levels cannot be satisfactorily described by simple textbook quantization rules.

II. MODEL

The present model Hamiltonian consists of a one-dimensional chain of s-like orbitals, treated in the tight-binding approximation, with nearest-neighbor interactions only,

$$H=\sum_n \left(\varepsilon_n|n\rangle\langle n|+V_{n,n+1}|n\rangle\langle n+1|+V_{n+1,n}|n+1\rangle\langle n|\right). \tag{1}$$

A finite chain segment emulates a double-barrier quantum-well structure either sandwiched by two semi-infinite contact chains (open system) or embedded by infinite barriers (isolated structure). Figure 1 (top panel) shows the ''bulk'' repulsive binary alloy attached to contacts in order to study transmission properties. Figure 2 (top panel) represents the double-barrier quantum-well structure, where the well is constituted by a short repulsive binary-alloy segment. The well material is a so-called repulsive binary alloy,[13,14] where the bond between one of the atomic species is inhibited, introducing short-range order: in a chain of A and B sites, only A-A and A-B nearest-neighbor bonds are allowed.

The introduction of this short-range order leads to delocalization of states in the disordered chain.[13,14] The well layer is then characterized by the degree of disorder (ordered or with uncorrelated or correlated disorder) and the concentration of B-like sites, which is related to the probability P_B of a B-like site to be the next one in generating a particular chain configuration. All results shown here are for $P_B=0.5$, corresponding to an effective concentration of B-like sites of $N_B \approx 0.3$. Disorder is straightforwardly introduced by randomly assigning A and B sites, according to the constraints on bonding and concentration mentioned above.

The problem of the transmission probability through the chains and the DBDQW can be exactly solved numerically, within the given model. We apply the Hamiltonian above to the total wave function, which yields, in principle, an infinite set of equations relating the local projections (of the wave function) on site n to the first-neighbor sites. From these, a new set of equations may be generated relating directly the projection on site l on the left of the DBDQW, to the projection on a site r to the right,

$$(E-\varepsilon_l')|l\rangle = V'|r\rangle + V_{l-1,l}|l-1\rangle, \tag{2}$$

$$(E-\varepsilon_r')|r\rangle = V'|l\rangle + V_{r,r+1}|r+1\rangle, \tag{3}$$

where E is the energy and primed quantities are obtained from the solution for the DBDQW subset, by the recursion method. The complete set of equations is kept finite by defining transfer matrices for the contacts $|l-1\rangle = T_l|l\rangle$ and $|r+1\rangle = T_r|r\rangle$. In this case, $|l\rangle$ is an incoming plus a reflected wave and $|r\rangle$ is the transmitted wave.[23] The wave function, and hence the probability density, is easily calculated within the same formalism. Since we are simulating disordered systems, averages over hundreds of configurations are undertaken.

The atomic site energies used throughtout this work are $\epsilon_A=0.3$ eV, $\epsilon_B=-0.3$ eV, and the hopping parameters are $V_{AA}=-0.8$ eV between A-like sites and $V_{AB}=-0.5$ eV between A-like and B-like sites for the well layer.[23] For the barriers, these parameters are $\epsilon_{br}=-0.025$ eV and $V_{br}=-0.15$ eV. We consider wells with up to $N_W=50$ sites and fixed barrier widths of $N_P=5$ sites. The contacts are chosen to be pure A-like chains. Changing the contact chains does not modify qualitatively the results shown below.[23] At interfaces we consider geometric averages of the hopping parameters. The results for transmission probabilities and probability densities for DBDQW structures are compared to energy spectra for similar systems embedded by infinite barriers. The VCA calculations have been made for the $A_{1-X}B_X$ alloy, with $X=0.3254$, which corresponds to an effective concentration of B-like sites for $P_B=0.5$.

III. RESULTS AND DISCUSSION

The properties of the ''bulk material'' are summarized in Fig. 1 (bottom panel) showing the localization lengths, $\lambda(E)=-2L/\ln[T(E)]$, of $L=100$ atomic sites long chains with correlated (continuous line) and uncorrelated (dashed line) disorder. As real systems are finite, states with localization length longer than the system are delocalizedlike, reaching transmission probabilities up to $T(E)\approx 1$. In this case there will be an energy range where the states are effectively

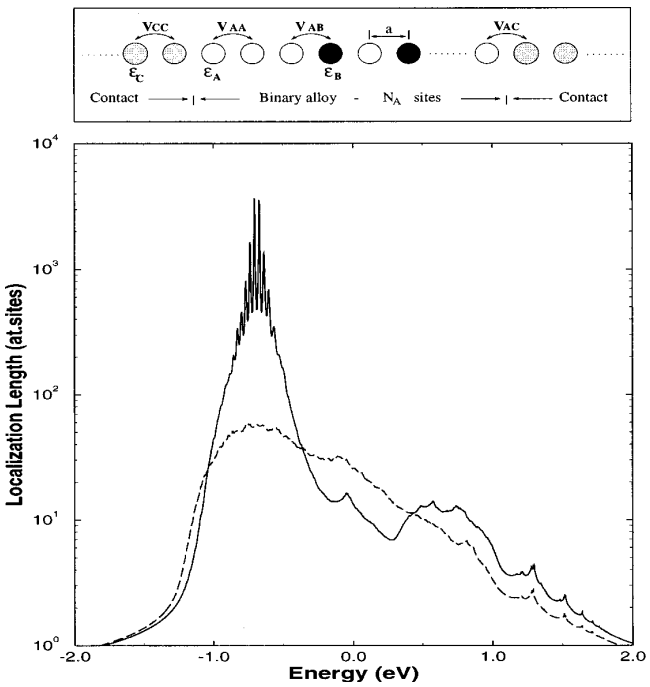

FIG. 1. Top panel: Disordered chains represents the ''bulk'' of a binary alloy. Bottom panel: Localization length as a function of energy for finite binary repulsive chains (100 sites) with correlated (continuous line) and uncorrelated (dashed line) disorder.

delocalized. For the correlated disorder case, continuous line in the bottom panel of Fig. 1, this energy range can be identified by the smoothness and oscillatory behavior of the localization length due to interference effects of these extended states. For the uncorrelated case (dashed line), this band of delocalized states is not observed.

Having in mind these properties of the ''bulk material,'' we turn now to the central question of the work: how quantum confinement effects can be characterized in quantum wells with this model of disorder. There are basically two kinds of structures in order to make the spectroscopy of quantized states due to spatial confinement: double barrier quantum wells embedded by contacts and quantum wells defined by thick barriers, for tunneling and optical spectroscopies, respectively. The present work is concerned with both situations. Since we are looking for quantum size effects, the barriers will sandwich short well-like chain (repulsive binary-alloy) segments.

Figure 2 shows transmission probabilities for a correlated (a) and an uncorrelated (b) DBDQW where the wells are $N_W=33$ sites wide. Figure 2(a) shows clear resonances in the transmission probability, in spite of disorder, in the energy range where the bulk chain presents delocalized states, as can be seen in Fig. 1. However, for the same energy range in the uncorrelated case, no signatures of such resonances are present. Transmission probability peaks are usually associated to quantum confinement effects in ordered quantum well systems.[25] In the present context they only occur when the well material shows a ''delocalization energy window.'' A detailed inspection of these results, having in mind Fig. 1, shows that resonances appear at energy ranges where the bulk material presents states with a localization length that exceeds the quantum well width by at least a factor of three.

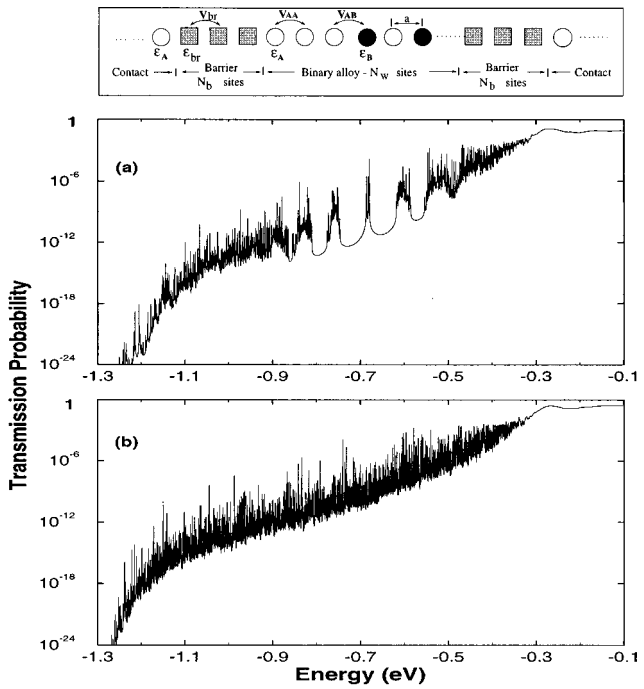

FIG. 2. Top panel: The double-barrier quantum-well structure. Bottom panel: Transmission probability as a function of energy for DBDQW's with $N_W=33$ and $N_P=5$ sites, considering (a) correlated and (b) uncorrelated disorder.

However, these resonances have their peak values drastically suppressed, as can be seen in Fig. 2(a), where the best resolved resonance reaches $T(E)\approx 10^{-6}$. Transmission probability resonance values close to unity occur only for symmetrical double-barrier quantum-well structures. Asymmetries in the structure may reduce this value by many orders of magnitude.[25] The origin of these asymmetries in ordered quantum wells is normally related to applied external fields or unequal barriers. In the present case, the asymmetry is intrinsically present in the well due to the disorder. For a given value of P_B, very few alloy configurations are symmetric relative to the well center and the weight of their resonances is low due to the averaging procedure. On the other hand, any potential profile, independent of asymmetries, may show transmission probability maxima close to unity for energies above the barrier. For the present case, the barrier top is given by $\epsilon_{br}-2V_{br}=-0.325$ eV. Indeed, relatively high transmission probabilities, $T(E)\approx 0.1$, are seen for both correlated and uncorrelated disorder, Fig. 2(a) and Fig. 2(b), for energies above -0.3 eV.

In order to elucidate the nature of the resonances in the transmission probability, and their relation to quantum confinement effects, a careful mapping of the energy spectra of double-barrier quantum wells embedded by infinite barriers is necessary. In Fig. 3, the energy spectra as a function of quantum-well width are shown. For each well width, ten disordered configurations are displayed in order to visualize the energy fluctuations due to disorder. The well width is varied from $N_W=20$ up to $N_W=50$ sites. Two clearly distinct regions are identified: large fluctuations in the energy ranges where the states are localized and a strong suppression of the fluctuations in the ''delocalization window,'' which can be defined around the energy for maximum λ. In the present

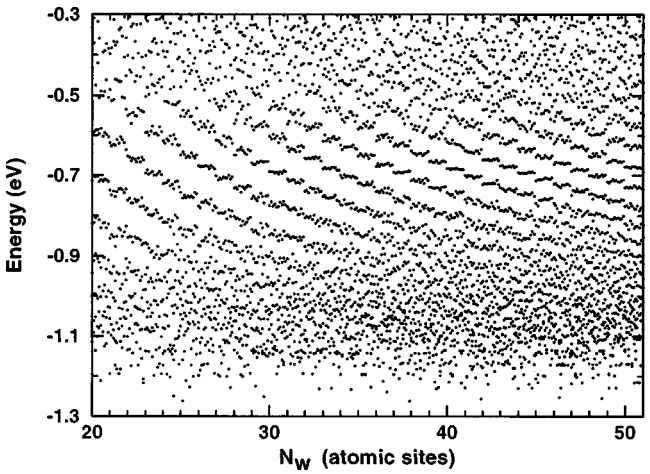

FIG. 3. Energy spectra of barrier-disordered well-barrier structure embedded by infinite barriers with correlated disorder as a function of the well width (N_W). There are ten realizations per width.

case, $E_{\lambda_{max}}\approx -0.7$ eV, independent of the well width. Actually this value agrees with the results shown in Fig. 1 for a repulsive binary-alloy chain segment $L=100$ atomic sites long in the absence of barriers. The position of the maximum localization length does not depend on the chain length. By increasing (decreasing) the well width, bona fide quantum-well levels with increasing (decreasing) quantum numbers are tuned into the ''delocalization window.'' The expected level blueshift with well width can now be followed as in ordered quantum wells, but only in this particular energy range. Indeed, for certain well widths, these states are almost perfectly aligned for the energy scale of the figure. It should be noticed that these states, which appear at the same energy independent of the chain configurations, always have the same quantum number, as can be easily verified by just counting the states. This is a signature for quantum-well states, in spite of the disorder. In the present case, the resolved level near $E_{\lambda_{max}}$ for $N_W=50$ corresponds to the state $n=15$ and for $N_W=20$ to $n=6$.

The states at the bottom of the spectra shown in Fig. 3 are in the range of localized states, and their average energy also increases when the well width is reduced. This shift, however, is due to the states localized near the interface that are taken into account in the averaging procedure. The contribution of these states is clearly enhanced with further reduction of the well width. We stress here that the nature of this energy shift is completely different from the effects of quantum confinement. Therefore, the shift of the fundamental state in disordered quantum wells cannot be taken solely as evidence of quantum confinement.[26]

Further, we expect that the envelope functions associated to these quantum-well energy levels present clear symmetry properties. This is confirmed by the correct correlation between the quantum number and the number of nodes that appear in the averaged probability density. Figure 4 shows averaged probability densities for resonances in the transmission probability through a DBDQW structure near $E_{\lambda_{max}}$ for different well widths: $N_W=20$ (a), $N_W=23$ (b), $N_W=27$ (c), and $N_W=30$ sites (d), corresponding to $n=6$, $n=7$, $n=8$, and $n=9$ states, respectively. The related probability densi-

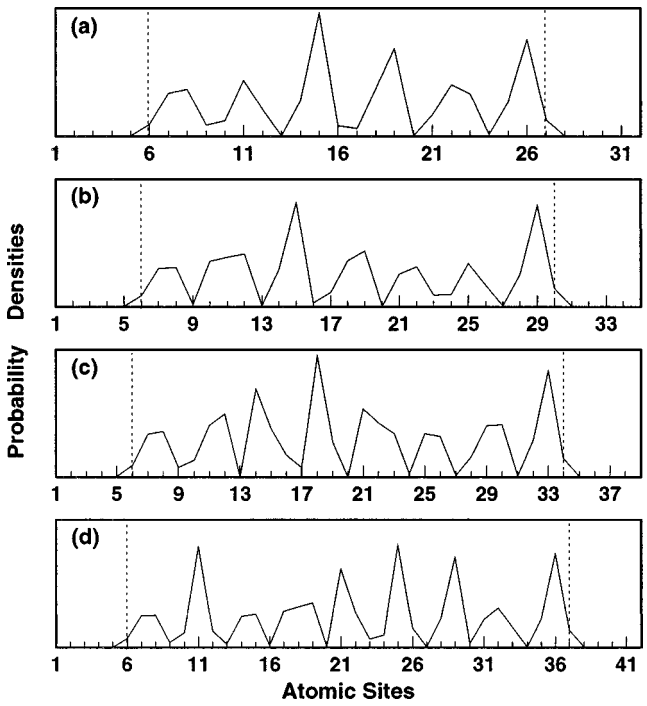

FIG. 4. Probability densities along the atomic sites of a DBDQW structure: (a) $N_W=20$ at $E=-0.716$ eV, (b) $N_W=23$ at $E=-0.698$ eV, (c) $N_W=27$ at $E=-0.709$ eV, and (d) $N_W=30$ at $E=-0.696$ eV.

ties show, indeed, $n-1$ nodes, identifying bona fide envelope functions of quantum-well bound states. Superimposed to these general features, there are still minor fluctuations related to the underlying disorder.

Up to this point quantum-well states in the ''delocalization energy window'' have been undoubtedly characterized. Nevertheless, it is still important to inspect how the eigenstates of a given quantum well evolve when the energy range of delocalized states is approached from the bottom of the spectrum, where the states are clearly localized. Figure 5(a) shows the probability density for the eigenstates of a single configuration of a double-barrier quantum well $N_W=30$ sites wide embedded by infinite barriers. The states labeled by *1*, *2*, *3*, and *4*, corresponding to $n=1$ to $n=4$, are clearly localized. On the other hand, the states labeled by *7*, *8*, and *9* ($n=7$ to $n=9$) show well-defined quantum-well envelope probability densities. However, if an average is made over many configurations, the localized states are apparently extended over the entire well as can be seen in Fig. 5(b) for the average probability densities of the same states of Fig. 5(a). We recall that the averaged probability densities of localized states in the quantum well, *1′*, *2′*, *3′*, and *4′* in Fig. 5(b), have no clear symmetry, and no resonances in the transmission probability are associated to these localized states. Therefore, the distinction between quantum-well states (at energies with localization length exceeding many times the quantum-well width) and the localized states is always very clear, independent of the averaging procedure.

A final point, to be investigated, is the possibility of establishing a quantization rule, as well as a mapping of the problem on a simple effective model, such as the effective-mass approximation in the context of crystalline semiconductors-based heterostructures.[1] A disordered chain

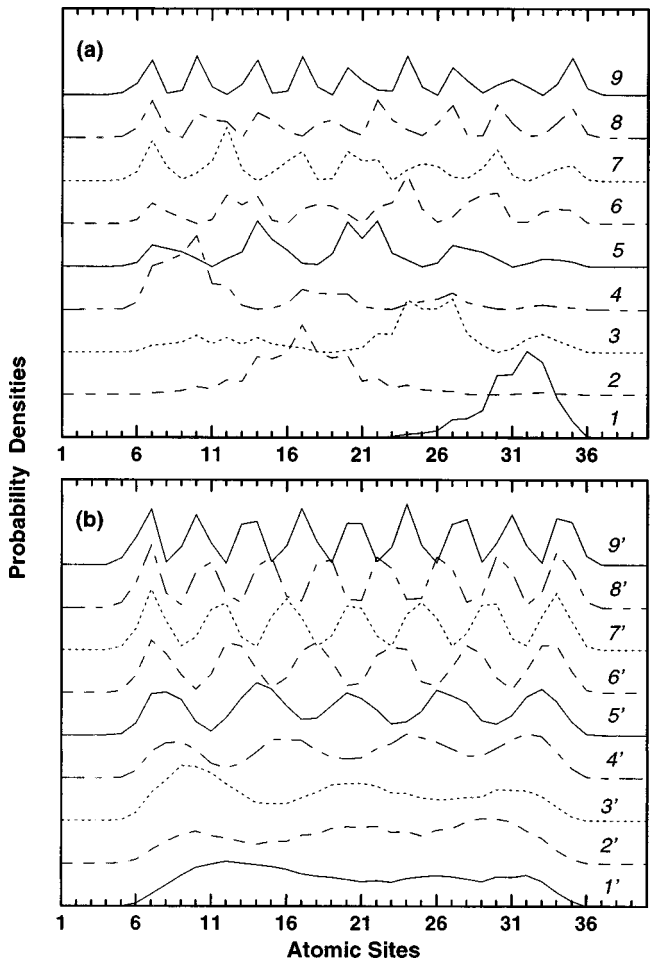

FIG. 5. Probability densities along a disordered well, $N_W=30$ sites wide, embedded by infinite barriers, with correlated disorder. (a) One configuration and (b) average over 50 configurations. See the text for details.

can be seen as a sequence of clusters with memory of the band structures of ordered chains where these clusters are the unit cells.[23] In the present case, our model with correlated disorder has two clear limits: a quantum well made only of *A*-like sites and a quantum well made of an *A*-*B* ordered alloy. These cases correspond to $P_B=0.0$ and $P_B=1.0$, respectively. Both limits are possible configurations for short chains, since they can be seen as clusters of a longer correlated disordered chain, and may shed some light on the quantization rules for our model disordered quantum well. In Fig. 6(a) we show the energy of the $n=10$ state as a function of quantum-well width in units of atomic sites, N_W. Open triangles (squares) are for the pure *A*-like sites and ordered *A*-*B* alloy cases, respectively. Dotted lines are only guides for the eyes. Dark circles represents the average value of the $n=10$ eigenstates over many disordered quantum-well configurations as a function of N_W, while the error bars represent the heterogeneous broadening of these states. We see that the $n=10$ state shows the smallest broadening at the crossing of the curves representing the ordered cases. Here we have the delocalization effect of long repulsive binary alloy chains translated to a short chain embedded by barriers situation: crossing of all energy curves, as a function of N_W, for a given quantum-well eigenstate, n, at exactly the same

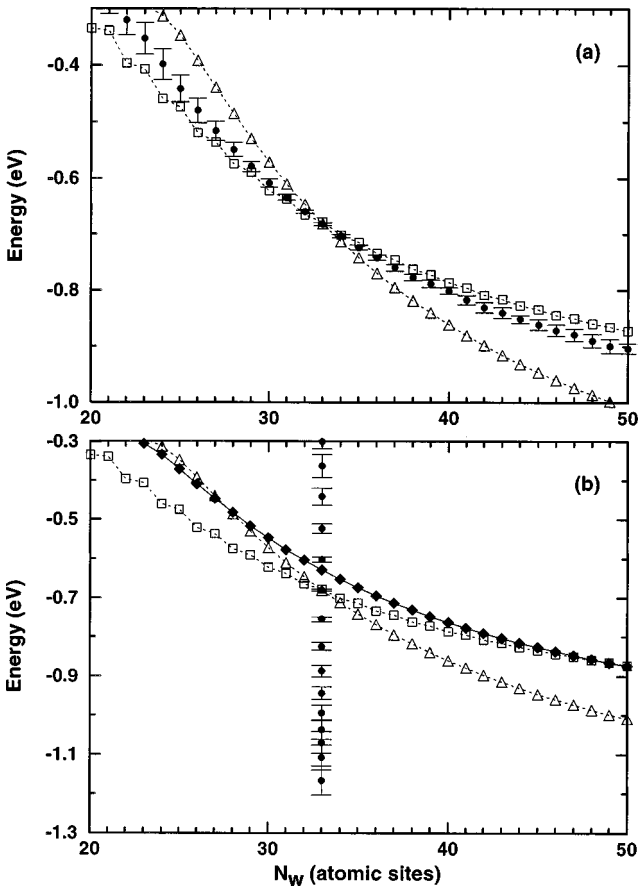

FIG. 6. Dependence of the $n=10$ state on the well width (N_W) for a double-barrier quantum-well structure embedded by infinite barriers. (a) Mean value (dark circles) and heterogeneous broadening of these states (error bars) over many configurations. Open circles are for a quantum well made only of A-like sites and open squares are for one made of an A-B ordered alloy. (b) Diamonds are for a VCA calculations for the $n=10$ state. Open circles and squares the same as (a). Dark circles (error bars) are the mean values (heterogeneous broadening) of bounded levels of a DBDQW $N_W=33$ sites wide.

point, irrespective to the quantum-well configuration, would represent an infinite localization length. However, since the quantum-well width cannot be varied continuously, even a bona fide quantum-well state will generally show a finite heterogeneous broadening. From these results it is straightforward that the crossings of the corresponding curves for higher (lower) quantum-well eigenstates occur around higher (lower) values of N_W, but close to the same energy value, namely $E_{\lambda_{\max}} \approx -0.7$ eV.

Considering this model quantum well, now with infinite barriers, the best defined confined state can be estimated analytically. One can easily find which state of the pure A-like sites chain [given by $E(K)=E_A+2V_{AA}\cos(Ka)$, where $K=\pi n/(N_W+1)a$ and a is the lattice parameter] has the closest energy to the energy of maximun localization length for a repulsive binary alloy that can also be obtained analytically.[23] On the other hand, the broadening of the state cannot be estimated analytically. More important is that other states are also well defined quantum-well bond states for each quantum-well width, as can be seen in the resonances for the $N_W=33$ case in Fig. 2(a), and from the spectra in Fig. 3. This broadness of the ''quantization window'' is an involved and subtle question deserving further work. Concerning the mapping of the problem on a simple effective model, Fig. 6(b) shows the ordered limit cases of Fig. 6(a) compared to the prediction given by a VCA chain for the $n=10$ state (filled diamonds). The filled circles are the mean value for the bounded states for a correlated disordered well $N_W=33$ sites wide. Clear discrepancies are observed: the energy positions of quantum levels, given by the VCA approximations, are not in agreement with the numerical results. This can be explained as due to the fact that the VCA does average the lattice potential, not taking into consideration the correlations between nearest neighbors, which plays a paramount role in the delocalization of states and consequently in the quantum confinement effects.

IV. CONCLUSIONS

The general trend observed in this work is that disordered quantum wells do show bona fide levels due to quantum confinement in energy ranges where the localization lengths of the well material are at least three times longer than the well width. This results are in agreement with the view of a quantum-well bond state resulting from multiple constructive interference of the wave function.[25] Nevertheless, the establishment of simple quantization rules is an involved task and the full understanding of the electronic properties of such systems needs a treatment beyond analytical estimations. Moreover, since the ''delocalization window'' defines a ''quantization window,'' where the levels are well resolved in energy, there will also be a gap between the localized states and the bound (extended) states near the edges of the ''quantization window.'' [6]

It is rather surprising that the ''delocalization window'' selects a few states to be quantized, regardless of the strong energy fluctuations that occur for all others. An interesting related result is that identifying the quantum number of a bona fide level due to quantum confinement in a DBDQW structure, the number of localized states lower in energy is automatically given. Embodied in this results is the prediction that disordered systems with mobility edges should show quantum states due to spatial confinement in the range of delocalized states. The present results also give a hint of how these effects could be measured. The observed quantized states could be better resolved in optical experiments than in resonant tunneling spectroscopy. This can be seen by comparing Figs. 2 and 3. Although resonances are well defined in the transmission probability, they are very weak, due to the unavoidable asymmetries[25] introduced by disorder. On the other hand, the clear resolution of the quantized states shown in Fig. 3, and the well behaved corresponding envelope functions, Fig. 4, suggest that optical modulation spectroscopy should be an appropriate tool to investigate this phenomenon.

The aim of the present work is not concerned with quantitative comparisons with related experimental results. Nevertheless, the energy and length scales are the same as those of real quantum well systems.[1] If the lattice parameter of the present chain is taken to be a typical interatomic distance of

real systems, $N_W \approx 50$, for example, would represent well widths of the order of 10 nm.

Implicit in the results shown here is the fact that effective models, such as VCA, do not work for systems where the effective delocalization plays an important role in the quantum confinement. Since mean-field models do not take into account the correlations responsible for a ''delocalization window,'' they cannot show which eigenstate is quantum confined in the well or simply localized due to the disorder.

Note added in Proof. Similar results, concerning the inadequacy of effective models, have been recently discussed by Dargam, Capaz, and Kioller[27] in the context of alloy disorder effects on AlGaAs/GaAs quantum wells.

ACKNOWLEDGMENTS

The authors would like to acknowledge financial support from CNPq and FAPESP, Brazil, as well as partial support from Colciencias, Colombia.

*Present address: Departamento de Física, Universidad de los Andes, A.A. 4976, Santafe de Bogota, Colombia.

[1] See, e.g., G. Bastard, *Wave Mechanics Applied to Semiconductor Heterostructures* (Les éditions de Physique, Paris, 1992).
[2] S. Miyazaki, Y. Ihara, and M. Hirose, Phys. Rev. Lett. **59**, 125 (1987).
[3] I. Pereyra, M. P. Carreño, and F. Alvarez, J. Non-Cryst. Solids **110**, 175 (1989).
[4] Gen Chun, V. E. Kaznacheev, and A. E. Yunovich, Superlattices Microstruct. **9**, 191 (1991).
[5] K. Hattori, T. Mori, H. Okamoto, and Y. Hamakawa, Phys. Rev. Lett. **60**, 825 (1988).
[6] Z. Li and W. Pötz, Phys. Rev. B **47**, 6509 (1993).
[7] N. Porras-Montenegro and E. V. Anda, Phys. Rev. B **43**, 6706 (1991).
[8] M. E. Raikh, S. D. Baranovskii, and B. I. Shklovskii, Phys. Rev. B **41**, 7701 (1990).
[9] P. A. Schulz and C. E. T. Gonçalves da Silva, Phys. Rev. B **38**, 10 718 (1988).
[10] Raphael Tsu, J. Non-Cryst. Solids **114**, 708 (1989).
[11] Y. L. Jiang and H. L. Hwang, Appl. Surf. Sci. **48/49**, 392 (1991).
[12] J. C. Flores, J. Phys.: Condens. Matter **1**, 8471 (1989).
[13] D. H. Dunlap, H-L. Wu, and P. W. Phillips, Phys. Rev. Lett. **65**, 88 (1990).
[14] H-L. Wu, W. Goff, and P. Phillips, Phys. Rev. B **45**, 1623 (1992).
[15] A. K. Sen and S. Gangopadhyay, Physica A **186**, 270 (1992).
[16] P. K. Datta, D. Giri, and K. Kundu, Phys. Rev. B **47**, 10 727 (1993).
[17] X. Chen and S. Xiong, Phys. Lett. A **179**, 217 (1993).
[18] S. N. Evangelou and A. Z. Wang, Phys. Rev. B **47**, 13 126 (1993).
[19] J. C. Flores and M. Hilke, J. Phys. A **26**, L1225 (1993).
[20] A. Sánchez, E. Maciá, and F. Domínguez-Adame, Phys. Rev. B **49**, 147 (1994).
[21] A. Sánchez, F. Domínguez-Adame, G. Berman, and F. Izrailev, Phys. Rev. B **51**, 6769 (1995).
[22] J. Heinrichs, Phys. Rev. B **51**, 5699 (1995).
[23] R. Rey-Gonzalez and P. A. Schulz, Phys. Rev. B **54**, 7103 (1996).
[24] C. M. Soukoulis, M. J. Velgakis, and E. N. Economou, Phys. Rev. B **50**, 5110 (1994).
[25] B. Ricco and M. Y. Azbel, Phys. Rev. B **29**, 1970 (1984).
[26] M. Beaudoin, M. Meunier, and C. J. Arsenault, Phys. Rev. B **47**, 2197 (1993).
[27] T. G. Dargam, R. B. Capaz, and B. Koiller, Phys. Rev. B. **56**, 9625 (1997).